




ORIGINAL ARTICLE

TET1 upregulation drives cancer cell growth through aberrant enhancer hydroxymethylation of HMGA2 in hepatocellular carcinoma

Kiyokazu Shirai^{1,2} | Genta Nagae¹  | Motoaki Seki^{1,3} | Yotaro Kudo⁴ |
 Asuka Kamio^{1,5} | Akimasa Hayashi^{1,6} | Atsushi Okabe^{1,3} |
 Satoshi Ota¹ | Shuichi Tsutsumi¹ | Takanori Fujita¹ | Shogo Yamamoto¹  |
 Ryo Nakaki¹ | Yasuharu Kanki⁷ | Tsuyoshi Osawa⁸ | Yutaka Midorikawa⁹  |
 Keisuke Tateishi⁴ | Masao Ichinose^{2,10} | Hiroyuki Aburatani¹

¹Genome Science Division, Research Center for Advanced Science and Technology, The University of Tokyo, Tokyo, Japan

²Department of Gastroenterology, Wakayama Medical University, Wakayama, Japan

³Department of Molecular Oncology, Graduate School of Medicine, Chiba University, Chiba, Japan

⁴Department of Gastroenterology, Graduate School of Medicine, The University of Tokyo, Tokyo, Japan

⁵Laboratory of Genetics, Department of Biological Sciences, The University of Tokyo, Tokyo, Japan

⁶Department of Pathology, Kyorin University Faculty of Medicine, Mitaka, Japan

⁷Division of Clinical Medicine, Faculty of Medicine, University of Tsukuba, Tsukuba, Japan

⁸Division of Integrative Nutriomics and Oncology, Research Center for Advanced Science and Technology, The University of Tokyo, Tokyo, Japan

⁹Department of Digestive Surgery, Nihon University School of Medicine, Tokyo, Japan

¹⁰Faculty of Medicine, Teikyo University, Tokyo, Japan

Correspondence

Genta Nagae, Genome Science Division, Research Center for Advanced Science and Technology, The University of Tokyo, 4-6-1 Komaba, Meguro-ku, Tokyo 153-8904, Japan.

Email: nagaeg-tky@umin.ac.jp

Funding information

National Institute of Biomedical Innovation; Japan Science and Technology Agency, Grant/Award Number: 24221011; Ministry of Education, Culture, Sports, Science and Technology, Grant/Award Number: 25860521

Abstract

Ten-eleven translocation 1 (TET1) is an essential methylcytosine dioxygenase of the DNA demethylation pathway. Despite its dysregulation being known to occur in human cancer, the role of TET1 remains poorly understood. In this study, we report that TET1 promotes cell growth in human liver cancer. The transcriptome analysis of 68 clinical liver samples revealed a subgroup of *TET1*-upregulated hepatocellular carcinoma (HCC), demonstrating hepatoblast-like gene expression signatures. We performed comprehensive cytosine methylation and hydroxymethylation (5-hmC) profiling and found that 5-hmC was aberrantly deposited preferentially in active enhancers. TET1 knockdown in hepatoma cell lines decreased hmC deposition with cell growth suppression. *HMGA2* was highly expressed in a *TET1*^{high} subgroup of HCC, associated with the hyperhydroxymethylation of its intronic region, marked as histone H3K4-monomethylated, where the H3K27-acetylated active enhancer chromatin state induced interactions with its promoter. Collectively, our findings point to a novel type of epigenetic dysregulation, methylcytosine dioxygenase *TET1*, which

This is an open access article under the terms of the Creative Commons Attribution-NonCommercial License, which permits use, distribution and reproduction in any medium, provided the original work is properly cited and is not used for commercial purposes.

© 2021 The Authors. *Cancer Science* published by John Wiley & Sons Australia, Ltd on behalf of Japanese Cancer Association.

promotes cell proliferation via the ectopic enhancer of its oncogenic targets, *HMGA2*, in hepatoblast-like HCC.

KEYWORDS

enhancer, epigenome profiling, hepatocellular carcinoma, hydroxymethylation, TET1

1 | INTRODUCTION

Epigenomic aberration is one of the hallmarks of cancer.¹⁻³ The global hypomethylation and promoter hypermethylation of cancer-related genes are frequently observed in human cancer cells. Genome-wide alterations of histone modifications also result in the disruption of gene expression networks.^{4,5} Recently, comprehensive analyses using genomic technologies have revealed altered epigenetic regulators, including DNA modifying enzymes,⁴ histone modifiers,⁵ and chromatin remodelers.^{6,7} The ectopic activation of epigenetic regulators can promote oncogenic phenotypes and play essential roles during carcinogenesis. Therefore, it is thought to be a potential target for anticancer therapeutics.^{8,9}

The ten-eleven translocation (TET) family of proteins, *TET1*, *TET2*, and *TET3*, encode 5-methylcytosine (5-mC) dioxygenases that convert 5-mC to 5-hydroxymethylcytosine (5-hmC).^{10,11} The enzymatic role of TET proteins of the mammalian DNA demethylation pathway suggests the involvement of epigenetic dysregulation in various human cancers.¹²⁻¹⁶ Recent years have seen an increase in research conducted on TET1, especially with regard to its role in stem cell maintenance.^{7,17-21} However, the role of aberrantly expressed *TET1* in human cancers remains poorly understood.²²

In this study, we focused on the upregulation of *TET1* in a subgroup of hepatocellular carcinoma (HCC). A functional assay using liver cancer cell lines revealed that the overexpression of TET1 promotes hepatoma cell proliferation. We performed a genome-wide mapping of 5-mC and 5-hmC for *TET1*-upregulated HCC and found that 5-hmC was significantly enriched in active enhancer regions. The methylation status of this regulatory region changes dynamically during hepatic differentiation. An oncogenic effector gene, *HMGA2*, which is epigenetically upregulated by ectopic *TET1* expression, was identified.

2 | MATERIALS AND METHODS

2.1 | Cell lines

The liver cancer cell lines HepG2 and Huh7 were obtained from the Cell Resource Center for Biomedical Research at Tohoku University and the Japanese Collection of Research Bioresources (Osaka, Japan), respectively. The cells were cultured in Dulbecco's modified Eagle medium (DMEM) (Life Technologies) supplemented with 10% fetal bovine serum (FBS) and penicillin/streptomycin.

2.2 | Clinical samples

HCC patients undergoing hepatectomy in the Hepato-Biliary-Pancreatic Surgery Division, Department of Surgery, Graduate School of Medicine, University of Tokyo were included in this study after providing informed consent. The surgical specimens were immediately cut into small pieces after resection, snap frozen in liquid nitrogen, and stored at -80°C .

2.3 | RT-qPCR

Total RNAs from cell lines and clinical tissue samples were isolated using TRIzol reagent (Invitrogen, #15596018) according to the manufacturer's instructions. One microgram of RNA was used for the generation of double-stranded cDNA with the SuperScript Double-Stranded cDNA Synthesis Kit (Invitrogen, #1197010) and analyzed by real-time PCR using SYBR Green. The expression levels of the examined genes were normalized to β -actin expression. The PCR conditions for each cycle were as follows: denaturation at 95°C for 15 seconds, annealing at 60°C for 30 seconds, and extension at 72°C for 20 seconds. The sequences of primers for *TET1*, *HMGA2*, and β -actin are listed in Table S1.

2.4 | Gene expression microarray

The genome-wide analysis of the mRNA expression levels using U133 plus 2.0 human expression array (Affymetrix) was performed as described previously.⁴ Briefly, $1\ \mu\text{g}$ of RNA was used for the generation of double-stranded cDNA with the SuperScript Double-Stranded cDNA Synthesis Kit (Invitrogen) according to the manufacturer's protocol.

2.5 | Immuno-dot blot assay

The genomic DNA of HepG2 or Huh7 cells was isolated by phenol/chloroform treatment and precipitated with 70% ethanol. The genomic DNA of the clinical tissue samples was isolated using the QIAamp DNA Mini kit (QIAGEN, #51304). All genomic DNA was denatured at 95°C for 5 minutes in the 5-hmC assay. The DNA samples were spotted onto a Hybond-N+ nylon membrane (GE Healthcare, #RPN1210B). The membranes were then cross-linked with UV at $0.18\ \text{J}/\text{cm}^2$ and blocked with 5% nonfat milk in Tris-buffered saline

containing 0.1% Tween-20 (TBS-T), followed by incubation with the antibodies against 5-mC (1:2000, Diagenode, #MAB-081-100) and 5-hmC (1:2000, Active Motif, #39769) at 4°C overnight. The membranes were then washed and probed with an appropriate HRP-conjugated secondary antibody (anti-mouse IgG, GE Healthcare, #NA9310V, or anti-rabbit IgG, GE Healthcare, NA9340V) and detected with the ECL Plus chemi-luminescence assay kit (Thermo Scientific, #1896426 A and B). To measure the relative amount of each sample, the same blot was stained with 0.02% methylene blue in 0.3 M sodium acetate (pH 5.2). Dot blot intensity was quantified by Multi Gauge software (version 3.0).

2.6 | Knockdown assay

For the knockdown of endogenous *TET1* or *HMGA2*, cells were transfected with 20 nM of specific small interfering RNAs (siRNAs) (Invitrogen) using Lipofectamine 2000 (Life Technologies, #11668-019). The sense sequences of the *TET1* and *HMGA2* siRNAs are listed in Table S2. Stealth RNAi™ siRNA negative control med GC duplex 2 (Invitrogen, #12935-112) was used as the control siRNA.

2.7 | Western blotting analysis

HepG2 or Huh7 cells were washed twice with ice-cold PBS and ruptured with RIPA buffer containing protease inhibitor (Roche, #1697498). Cell lysates were resolved by SDS-polyacrylamide gel electrophoresis (PAGE) and then transferred onto PVDF membranes. The membranes were blocked for 1 hour with 5% non-fat milk in TBS-T and incubated with anti-HaloTag antibody (Promega, #G928A), anti-*HMGA2* antibody (Active Motif, #61041), anti-V5 antibody (Invitrogen, #1305726), anti-nucleoporin antibody (BD Biosciences, #610498), or anti- β -actin antibody (Sigma, #A5441) at 4°C overnight. Membranes were washed for 20 minutes with TBS-T, probed with appropriate HRP-conjugated secondary antibodies, and detected with the ECL Plus chemi-luminescence assay kit (GE Healthcare).

2.8 | Growth assay

The control and transfected liver cancer cells were seeded at a density of 3 or 4 $\times 10^3$ cells/well in 96-well plates, respectively. Viable cells were counted using a cell counting kit-8 (Dojindo, #CK04) at 1, 3, 5, and 7 days after transfection.

2.9 | Overexpression assay

For the overexpression of *TET1*, the cells were transfected with HaloTag-h*TET1* (Promega), which contains full-length human *TET1*. HaloTag control vector (Promega, #G6591) was used as a negative

control. For the overexpression of *HMGA2*, cells were infected with pLenti6.3/V5-h*HMGA2*, which contains full-length human *HMGA2*. Full-length of h*HMGA2* was amplified by PCR and subcloned into a pLenti6.3/V5-DEST lentiviral vector (Invitrogen). To package the lentivirus, 293T cells were cotransfected with the packaging plasmid, psPAX2 and pMD2.G, and a pLenti6.3/V5-DEST plasmid containing the h*HMGA* or LacZ. pLenti6.3/V5-LacZ was used as a negative control. All constructs were verified by Sanger sequencing.

2.10 | Chromatin immunoprecipitation (ChIP)

Chromatin immunoprecipitation using anti-H3K4 trimethylation (H3K4me3) rabbit polyclonal antibody (Active Motif, #39159) and mouse monoclonal antibodies against anti-H3K4 monomethylation (H3K4me1) and anti-H3K27 acetylation (H3K27ac) (kindly gifted by Dr Hiroshi Kimura, Osaka University²³) was performed as previously reported.²⁴ Briefly, HepG2 and Huh7 cells were cross-linked with 1% formaldehyde for 10 minutes at room temperature, and the cross-linked cell lysates underwent ultrasonic fragmentation and were incubated with antibodies bound to protein A- and G-sepharose beads (GE Healthcare, #17127901 and #17061801) for H3K4me3 and magnet beads (Invitrogen, #112.02D) for H3K4me1 and H3K27ac at 4°C overnight. The beads were washed and eluted with elution buffer (0.5% SDS, 25 mM Tris-HCl, 5 mM EDTA). The eluates were treated with 1.5 μ g of pronase at 42°C for 2 hours and then incubated at 65°C overnight to reverse the cross-links. The immunoprecipitated DNA was purified by the QIAquick PCR Purification Kit (QIAGEN, #28106).

2.11 | Methylated and hydroxymethylated DNA immunoprecipitation (MeDIP and hmeDIP)

The genomic DNA of HepG2 or Huh7 cells was isolated by phenol/chloroform treatment and precipitated with 70% ethanol. The genomic DNA of clinical liver samples was isolated using the QIAamp DNA Mini kit (QIAGEN) according to the manufacturer's instructions. The genomic DNA was quantitated using the Qubit dsDNA HS kit (Invitrogen, #Q32854). Briefly, 20 μ g (hmeDIP) or 2 μ g (MeDIP) of genomic DNA from the cell lines and 5 μ g of genomic DNA from the clinical samples were sonicated and denatured at 95°C for 5 minutes. Fragmented DNA was incubated with 4 μ L of anti-5-mC antibody (Diagenode) or 4 μ L anti-5-hmC antibody (Active Motif) at 4°C for 3 hours and bound to protein A- and G-sepharose beads at 4°C for 1 hour. The beads were washed twice by wash buffer 1 (20 mM Tris-HCl, 2 mM EDTA, 150 mM NaCl, 1% Triton-X) and 2 (20 mM Tris-HCl, 2 mM EDTA, 300 mM NaCl, 0.1% SDS, 1% Triton-X) before eluting with the elution buffer (25 mM Tris-HCl, 10 mM EDTA, 0.5% SDS, 100 mM NaCl). The eluates were treated with 100 μ g of proteinase K at 55°C for 1 hour. The immunoprecipitated DNA was purified by phenol/chloroform treatment and precipitated with LiCl, glycogen, and 70% ethanol.

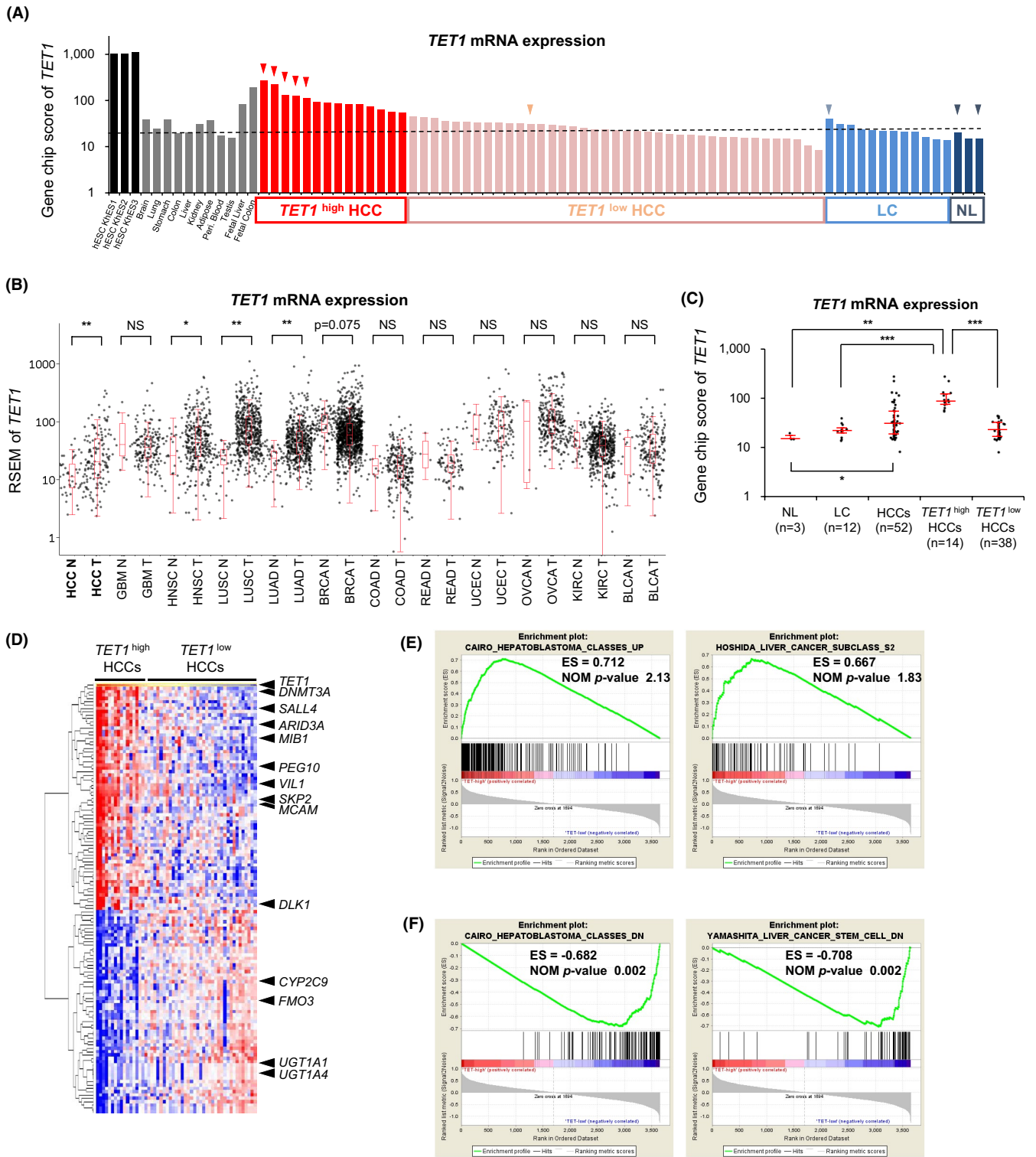


FIGURE 1 *TET1* is upregulated in hepatoblast-like HCC. A, *TET1* expression among hESCs, somatic tissues, and HCCs in expression microarray (U133 plus 2.0, Affymetrix). *TET1*: gene name, CXXC6; probe name, 228906_at. HCC, hepatocellular carcinoma; hESC, human embryonic stem cell; LC, liver cirrhosis (corresponding noncancerous liver); NL, normal liver. B, *TET1* expression among 12 types of cancer in RNA-seq data of TCGA project. BLCA, bladder urothelial carcinoma; BRCA, breast invasive carcinoma; COAD, colon adenocarcinoma; GBM, glioblastoma multiform; HCC, hepatocellular carcinoma; HNSC, head, and neck squamous cell carcinoma; KIRC, kidney renal clear cell carcinoma; LUAD, lung adenocarcinoma; LUSC, lung squamous cell carcinoma; N, nontumor; OVCA, ovarian serous cystadenocarcinoma; READ, rectal adenocarcinoma; T, tumor; TCGA, The Cancer Genome Atlas; UCEC, uterine corpus endometrial carcinoma. The black dot represents the *TET1* expression level (RSEM) of each case. Red line represents the median \pm quartile. C, *TET1* expression among clinical liver samples in expression microarray. Each dot represents the GeneChip score of *TET1* (228906_at). Red line represents the median \pm quartile. P-values were measured using the Mann-Whitney U-test in (B) and (C). * $P < .05$; ** $P < .01$; *** $P < .001$. D, Heatmap of the expression profiles using the probes which are highly correlated or inversely correlated with *TET1* expression among clinical liver samples. E and F, Enrichment plot showing the enrichment score for the gene sets upregulated (E) and downregulated (F) in *TET1*^{high} HCCs

2.12 | ChIP-, MeDIP-, and hmeDIP-sequencing (ChIP-, MeDIP- and hmeDIP-seq)

Sequencing was conducted on an Illumina Genome Analyzer GAIIx using Cluster Generation (version 2 and 4) chemistries, as well as Sequencing by Synthesis Kits (version 3 and 4). Data collection was performed using Sequencing Control Software (version 2.5 and 2.6). Real-Time Analysis (RTA) 1.5-1.8 was used for base calling. Genomic mapping of short reads was performed using the sequence_pair mode of ELAND in the Illumina CASAVA pipeline (version 1.5-1.8) (Table S3). Distribution of immunoprecipitated or enriched fragments was analyzed using model-based analysis for ChIP-seq (MACS).²⁵ Data were visualized using Integrative Genomics Viewer (IGV) (version 2.3.32).

2.13 | Multiplex targeted sequencing of bisulfite (BS)-treated amplicons

BS treatment of genomic DNA (200-250 ng) was performed by the EZ DNA Methylation-Gold Kit (ZYMO Research, #D5005) following the manufacturer's protocols. BS-converted DNA was amplified with 16 primer sets for the *HMGA2* enhancer region (Table S4) using KAPA HiFi HotStart Uracil + Ready Mix (KAPA Biosystems, #KK2801), and ligated with Illumina TruSeq adapters. The libraries of amplicons were generated by the Illumina TruSeq

TABLE 1 Clinicopathological characteristics of hepatocellular carcinoma (HCC) cases associated with *TET1* expression

Characteristic	<i>TET1</i> ^{high} HCCs (14/52)	<i>TET1</i> ^{low} HCCs (38/52)	P-value
Age, y	61 (32, 76) ^a	68 (48, 80) ^a	**0.003 ^b
Sex			
Male	12 (86%)	28 (74%)	**0.344 ^c
Female	2 (14%)	10 (26%)	
Etiology			
HBV	5 (36%)	12 (32%)	.779 ^c
HCV	9 (64%)	26 (68%)	
Tumor size, mm	45 (20, 100) ^a	30 (11, 120) ^a	**0.056 ^b
Differentiation			
Well	0 (0%)	9 (24%)	**0.014 ^c
Mod	10 (71%)	25 (68%)	
Por	4 (29%)	3 (8%)	
AFP, ng/mL	5770 (4, 145 972) ^a	13 (3, 9700) ^a	***<.001 ^b
DCP, mAU	106 (12, 5354) ^a	37 (10, 20 955) ^a	.358 ^b

Abbreviations: AFP, alpha-fetoprotein; DCP, des-gamma-carboxy prothrombin; HBV, Hepatitis B virus; HCV, Hepatitis C virus.

^aMedian (minimum, max).

^bP-value was measured by the Mann-Whitney *U* test.

^cP-value was measured by χ^2 test or Fisher's exact test.

P* < .01.; *P* < .001.

Nano DNA LT Sample Prep Kit (#15041757 and #15041759) according to the manufacturer's instructions, and quantified by the Agilent 2100 Bioanalyzer using High Sensitivity DNA chip. Multiplexed libraries were sequenced on the Illumina MiSeq, as 150-bp paired-end reads, following the manufacturer's recommendations. Sequenced reads were mapped to the top or bottom strand of the hg19 reference genome by Bismark 0.5.4 (Bowtie 0.12.2) using the default parameters. The uniquely mapped reads were processed to estimate the percentage of methylation. The methylation rate for each cytosine of the CG sites was estimated by dividing the number of C by the total number of C or T (read depth above 50).

2.14 | Chromatin conformation capture (3C) assay

A total of 1.8 million of HepG2 and Huh7 cells were transfected with siCTL or siTET1. Preparation of 3C templates were following the previous report (Rao et al²⁶) except for skipping the step of DNA end-repair and shearing. Briefly, 48 hours after transfection, cells were crosslinked by 1% formaldehyde for 10 minutes and quenched by 0.2 M glycine for 5 minutes. Cells were lysed in lysis buffer (10 mM Tris-HCl pH8.0, 10 mM NaCl, 0.2% Igepal CA630) containing 1 × cComplete, EDTA-free (Roche #11873580001) on ice for 15 minutes; then, chromatin was digested with EcoRI (NEB #R0101) at 37°C overnight. DNA ends were ligated with T4 DNA Ligase (NEB #M0202) at 4 hours, followed by protein digestion with Proteinase K (NEB #P8107) and crosslink reversal. DNAs were purified by phenol-chloroform extraction and ethanol precipitation; then, qPCR was performed. HepG2 and Huh7 cells with siCTL or siTET1 KD were used for 3C with the TaqMan 3C Chromosome Conformation Kits (Life Technologies, #4466151) according to the manufacturer's protocol. The sequences of the constant primer (forward) and the test primer (reverse) are listed in Table S5. A TaqMan probe was designed based on the negative strand DNA sequence located 23 bp upstream of the first EcoRI enzymatic digestion site. TaqMan quantitative real-time PCR was performed with SsoAdvancedTM Universal Probes Supermix (Bio-Rad, #172-5280) according to the manufacturer's protocol, using the following cycling conditions: denaturation at 95°C for 10 seconds and annealing and extension at 60°C for 60 seconds. The PCR products were purified using a QIAGEN quick gel purification kit (QIAGEN, #28106), and the sequence of each chimeric DNA was verified by Sanger sequencing (Figure S6). To normalize primer efficiency, control PCR templates were generated by digestion and random ligation of bacterial artificial chromosomes (BAC) containing *HMGA2* (Life Technologies, clone RP11-462A13). A total of 10 µg of BAC clone was digested with EcoRI (Toyobo, #ECO-153) and then ligated with T4 DNA ligase (NEB, #M0202S). The paired primers/probes designed for 3C-qPCR assay were tested on the random ligation product, which contained all possible chimeric DNA ligation products in equal molar concentrations.

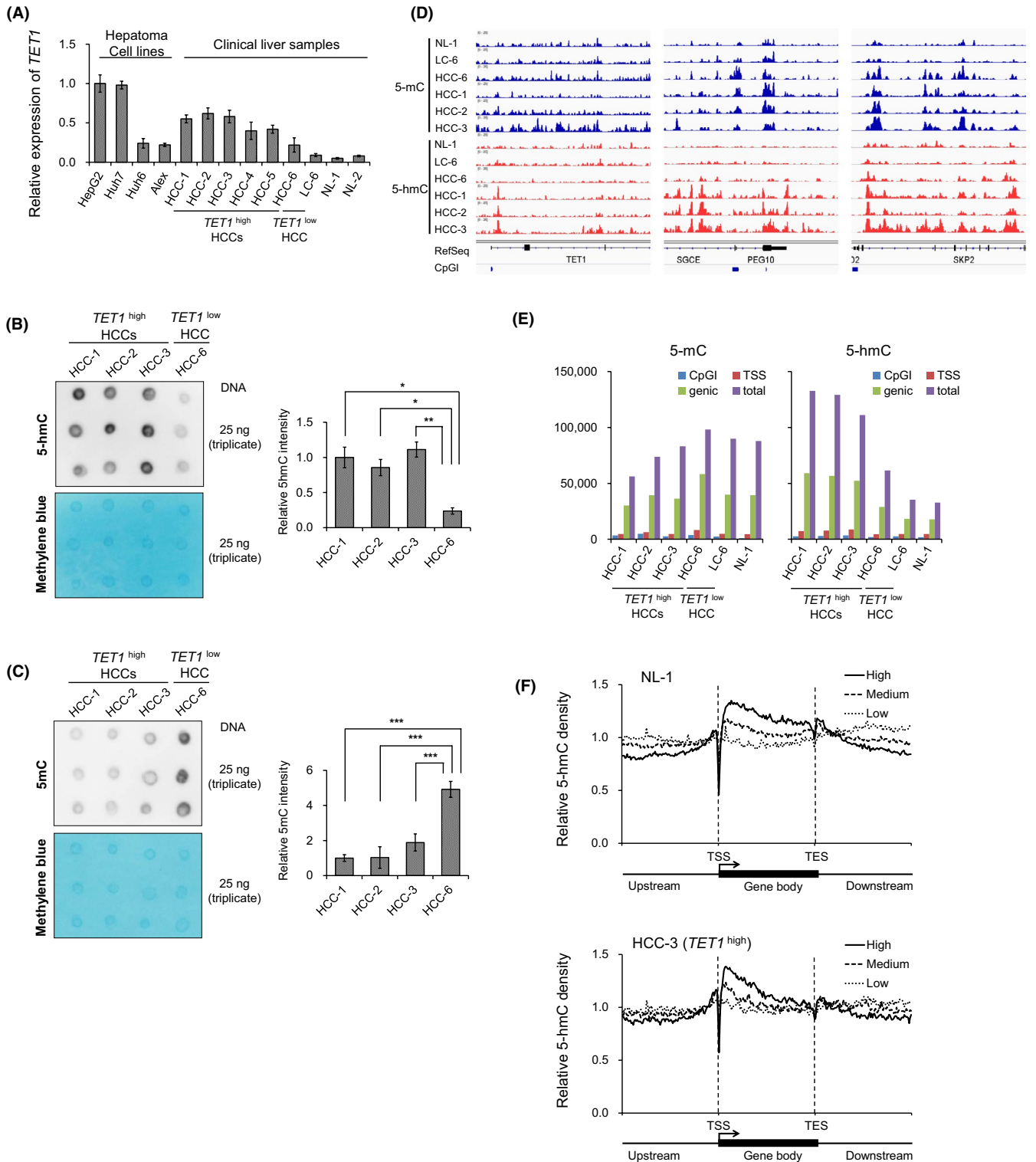


FIGURE 2 5-mC and 5-hmC profiles of clinical liver tissues. A, Relative *TET1* mRNA expression of hepatoma cells and clinical liver samples by RT-qPCR. B and C, Global 5-hmC (B) and 5-mC (C) levels in hepatocellular carcinomas (HCCs) quantified by immuno-dot blot assay. Left, dot blot images of triplicate experiments. The methylene blue staining is used as a loading control for total genomic DNA. Right, quantified dot blot intensity by Multi Gauge (version 3.0) software compared with HCC-1. Data are shown as the mean \pm SD of triplicate experiments. *P*-values are measured using Student's *t*-test in (B) and (C). **P* < .05; ***P* < .01; ****P* < .001. D, Genome-wide profiling of 5-mC (upper) and 5-hmC (lower) for clinical liver tissues (NL-1 as a normal liver; LC-6 as a noncancerous liver; HCC-6 as a *TET1*^{low} HCC; HCC-1, -2, -3 as *TET1*^{high} HCCs). Signal intensities are visualized using Integrated Genomics Viewer (IGV). E, The number of 5-mC-enriched regions (left) and 5-hmC-enriched regions (right) identified by MeDIP-seq and hmeDIP-seq, respectively. F, 5-hmC distributions relative to human RefSeq gene position by hmeDIP-seq according to the expression levels in clinical liver samples. TSS, transcription start site; TES, transcription end site. Expression level: high, GeneChip score >250; low, GeneChip score <25; medium, GeneChip score 25-250

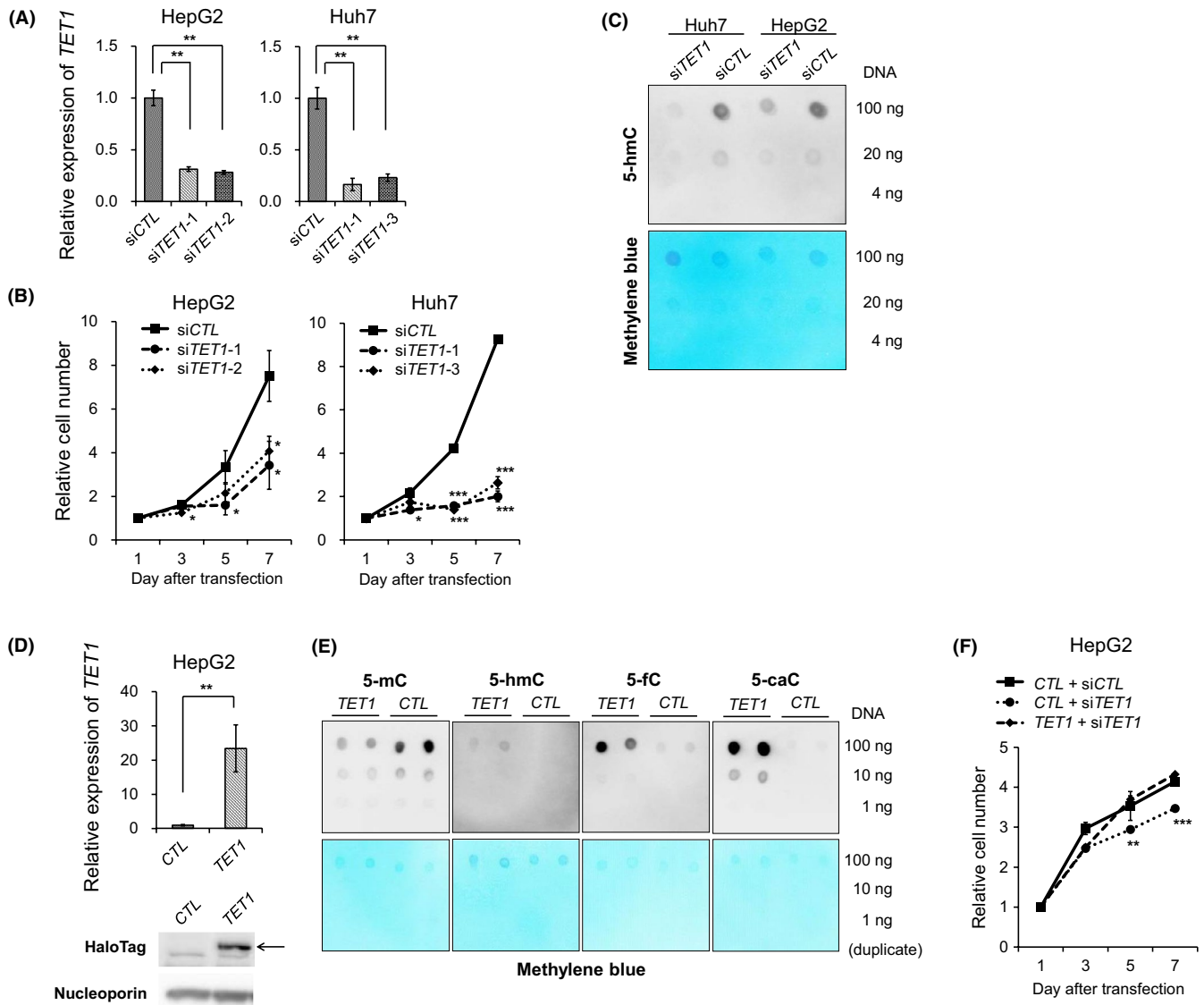


FIGURE 3 *TET1* knockdown inhibits proliferation of hepatoma cell lines. A, Relative *TET1* mRNA expression of hepatoma cells (HepG2 and Huh7) treated with control siRNA (siCTL) and *TET1* siRNA (siTET1-1, -2, and -3) by RT-qPCR. B, The tumor proliferation curves of HepG2 and Huh7 cells treated with siCTL and siTET1 transfection. C, Global 5-hmC levels in HepG2 and Huh7 cells treated with siCTL and siTET1 quantitated by immuno-dot blot assay. The methylene blue staining was used as a loading control for total genomic DNA. D, Forced overexpression of full-length *TET1* in HepG2 using HaloTag vector. CTL, untreated; *TET1*, treated with the Halo-*TET1* vector. Upper, relative *TET1* mRNA expressions by RT-qPCR compared with cells with CTL. Lower, *TET1* expression by Western blotting analysis using anti-HaloTag antibody and anti-Nucleoporin antibody. Arrow indicates the Halo-*TET1* proteins. E, Dot blot assays of methylcytosine oxidation using HEK293FT untreated (CTL) or treated with HaloTag vectors (*TET1*). Data are shown as duplicate experiments. The methylene blue staining is used as a loading control for total genomic DNA. F, The tumor proliferation curves of HepG2 and Huh7 cells treated with siCTL, siTET1, CTL, and *TET1*. Data in (A), (B), (D), and (F) are shown as the mean \pm SD from triplicate experiments. *P*-values were measured using Student's *t*-test in (A), (B), (D), and (F). **P* < .05; ***P* < .01; ****P* < .001

3 | RESULTS

3.1 | Clinicopathological features of *TET1*-upregulated HCC

To elucidate the dysregulation of *TET1* in the context of human liver cancer, we first examined its mRNA expression levels among clinical liver tissues using an expression microarray (U133 plus 2.0, Affymetrix). As shown in Figure 1A, *TET1* was upregulated in 14 of 53

HCCs (26.9%) compared with noncancerous liver tissues. In general, *TET1* is strongly expressed in human embryonic stem cells (hESC). In contrast, the expression level of *TET1* in somatic tissues, including the adult liver, was lower, which is consistent with the results of murine somatic tissues.¹⁷ Fetal liver and colon tissues showed relatively high levels of *TET1* expression, as well as *TET1*-upregulated HCCs. As for *TET2* and *TET3*, there was no significant difference between HCCs and noncancerous livers (Figure S1). Interestingly, the aberrant expression patterns of *TET1* mRNA were cancer type-dependent.

Large-scale transcriptome analyses ($n = 4175$, total) of The Cancer Genome Atlas (TCGA) research network are shown in Figure 1B. As previously reported by Hsu et al,¹³ *TET1* was relatively down-regulated in breast cancers because the epithelium in normal breast maintains high levels of expression. However, a significant upregulation of *TET1* was observed in lung cancers and head and neck squamous cell carcinomas, as well as HCCs.

To clarify the relationship between the expression level of *TET1* and the clinicopathological behaviors of HCCs, we investigated the clinical information of *TET1*-upregulated cases (*TET1*^{high} HCCs; greater than twofold of noncancerous liver tissues, $n = 14$) and the other cases (*TET1*^{low} HCCs, $n = 38$) (Table 1). As shown in Table 1, *TET1*^{high} HCCs were characterized by higher serum alpha-fetoprotein (AFP, $P < .001$), younger age ($P = .003$), and poorer pathological differentiation ($P = .014$) than *TET1*^{low} HCCs. No significant differences were observed with regard to gender, etiology, tumor size, or serum des-gamma-carboxy prothrombin (DCP) (Table 1 and Figure S2).

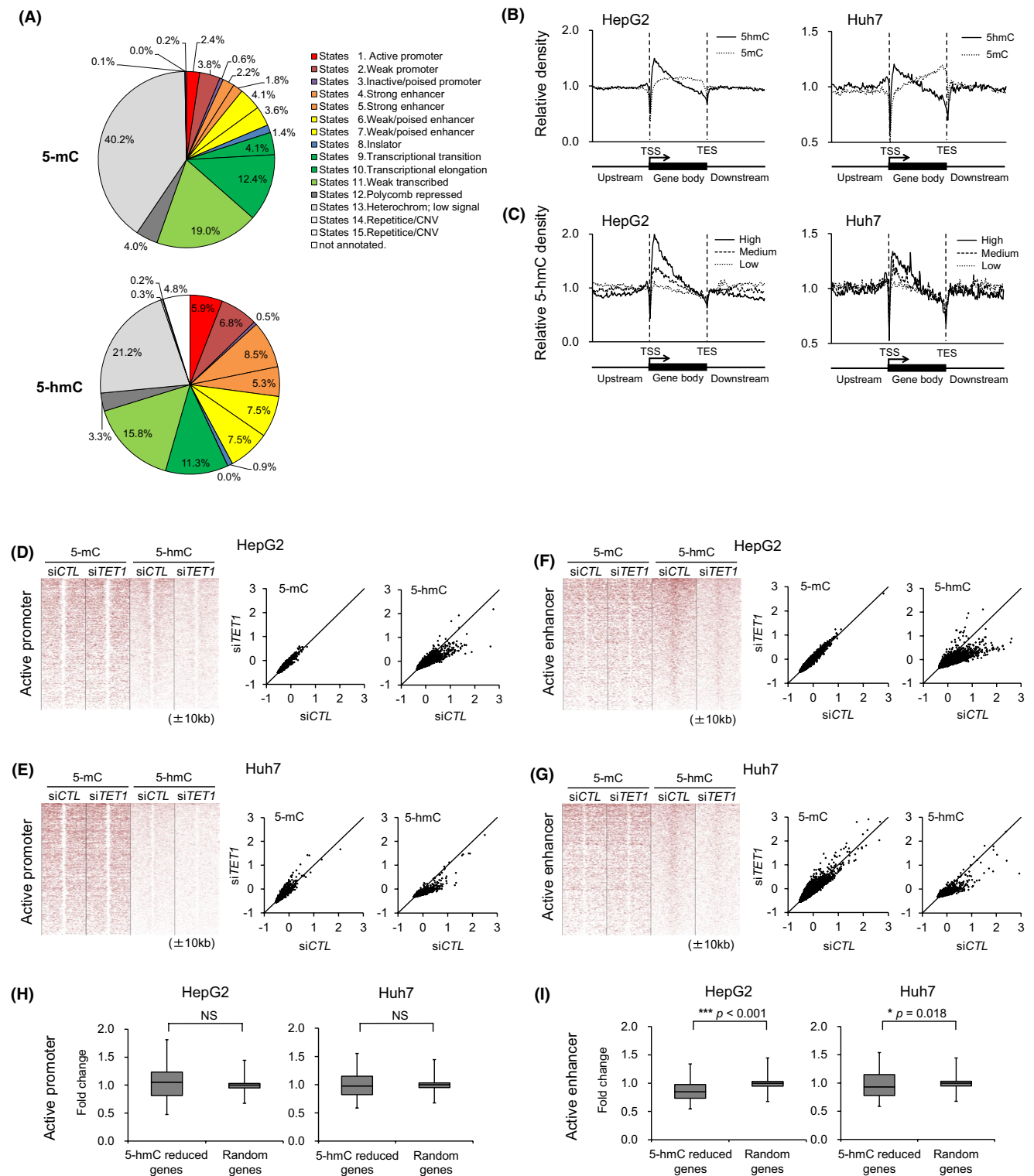
To further evaluate the expression profiles of *TET1*^{high} HCCs (Figure 1C), we performed hierarchical clustering analysis using probes whose expression patterns among 53 HCCs were highly correlated (correlation coefficient $\rho > .75$) or inversely correlated ($\rho < -0.5$) with the expression levels of *TET1*. Epigenetic regulators, such as *DNMT3A* and *ARID3A*, and two imprinted genes, *PEG10* and *DLK1*, were highly coexpressed with *TET1* (Figure 1D). The oncofetal gene *SALL4*²⁷ was also upregulated in *TET1*^{high} HCCs. On the contrary, genes specific for matured hepatocytes (*CYP2C9*, *FMO3*, *UGT1A1*, and *UGT1A4*) were downregulated. Gene Set Enrichment Analysis (GSEA) indicated that *TET1*^{high} HCCs have hepatoblast-like gene expression signatures. Cairo's gene sets,²⁸ representing overexpression in human hepatoblastoma (HBL), were found to overlap the most with the upregulated gene sets for *TET1*^{high} HCCs (Figure 1E). Hoshida's gene sets²⁹ for the G2 subclass, which is featured as hepatoblast-like HCC, were highly ranked with a significant nominal P -value ($P = .015$). The downregulated genes for *TET1*^{high} HCCs were well correlated with Cairo's gene sets downregulated in HBLs and with Yamashita's gene sets³⁰ downregulated in EpCAM-positive liver cancer stem cells (Figure 1F). These results indicate that *TET1*^{high} HCCs may be derived from premature hepatic progenitor cells with high levels of *TET1* expression.

3.2 | Genome-wide mapping of 5-hmC in clinical HCC samples reveals that 5-hmC is enriched at the transcriptional regulatory regions

The prevalence of *TET1* overexpression in HCCs raises an intriguing possibility that dioxygenase *TET1* may cause the aberrant hydroxymethylation of cytosine, which leads to malignant phenotypes via epigenetic disruption. To test this hypothesis, we first verified the mRNA levels of the *TET* family genes (Figure 2A, Figure S3A) and examined the total content of 5-hmC and 5-mC by immuno-dot blot assay (Figure 2B,C). Consistent with the GSEA result of *TET1*^{high} HCCs, *TET1* was highly expressed in the liver cancer cell line, HepG2 (Figure 2A), while 5-hmC might be globally increased in *TET1*^{high} HCC patients (Figure 2B). Conversely, the total content of 5-mC was decreased (Figure 2C).

To dissect the genome-wide distribution of 5-hmC and 5-mC in HCC, we performed a comprehensive profiling using a hmeDIP and MeDIP approach coupled with massively parallel sequencing (hmeDIP- and MeDIP-seq), respectively (Figure 2D). At the *TET1* gene locus, a prominent 5-hmC peak downstream from the transcription start site (TSS) was observed in *TET1*^{high} HCCs, which is consistent with reports that human *TET1* binds directly with its own promoter.¹⁵ Imprinted gene *PEG10* and cell cycle-related gene *SKP2* were also aberrantly hydroxymethylated in a *TET1*^{high} HCC-specific manner. As shown in Figure 2E, the total numbers of 5-hmC-marked regions were increased in *TET1*^{high} HCCs. Overall, 5-mC and 5-hmC were depleted at TSS regions but enriched on the gene-body regions in clinical liver samples (Figure 2F). Consistent with previous findings in murine ESCs,^{18,31,32} 5-hmC was preferentially enriched downstream of TSS (Figure 2F, Figure S3D). 5-mC was widely distributed in the gene-body region along the 3' ends (Figure S3C). With regard to the gene expression statuses, 5-hmC was more enriched downstream from the TSSs of highly expressed genes in clinical liver samples (Figure 2F). However, 5-mC enrichment showed no difference according to the gene expression levels (Figure S3C). Taken together, 5-hmC was enriched at the transcriptional regulatory region in *TET1*^{high} HCC.

FIGURE 4 Genome-wide distributions of 5-hmC and the effect of *TET1*-knockdown at the promoters and enhancers. A, Chromatin status of 5-mC-enriched regions (upper) and 5-hmC-enriched regions (lower) in HepG2 and Huh7 cells. B, 5-hmC and 5-mC distributions of HepG2 and Huh7 cells relative to human RefSeq gene position, respectively. C, 5-hmC distributions relative to human RefSeq gene position by hmeDIP-seq according to the expression levels in HepG2 and Huh7. Expression level: high, GeneChip score >250 ; low, GeneChip score <25 ; medium, GeneChip score 25–250. D–G, Heat map representation around active promoters and enhancers (± 10 kb) with enriched 5-mC and 5-hmC in HepG2 (D, F) and Huh7 (E, G) cells with siCTL and si*TET1*. Active promoters (D, E) are classified by genomic elements (H3K4me3 and H3K27ac positive). Active enhancers (F, G) are classified by genomic elements (H3K4me3 negative, and H3K27ac and H3K4me1 positive). The heat map is rank-ordered by 5-hmC levels of siCTL. Z-values of 5-mC or 5-hmC enrichments around active promoters (D, E) and active enhancers (F, G) (± 5 kb) in HepG2 and Huh7 cells with siCTL and si*TET1* are shown. Z-value indicates normalized deviations based on a normal distribution. H, Boxplot of the expression changes in HepG2 and Huh7 cells with siCTL and si*TET1* by expression microarray (U133 plus 2.0) at the active promoter of 5-hmC reduced genes (HepG2, 578 probes; Huh7, 517 probes) and randomly selected genes (each 1000 probe). 5-hmC-reduced genes show the genes whose 5-hmC sum score of hmeDIP-seq around active promoter (± 200 bp) is reduced to one-fifth by *TET1* knockdown. I, Boxplot of the expression changes in HepG2 and Huh7 cells with siCTL and si*TET1* by expression microarray (U133 plus 2.0) at active enhancer of 5-hmC-reduced genes (HepG2, 94 probes; Huh7, 118 probes) and randomly selected genes (each 1000 probe). 5-hmC-reduced genes show the genes whose 5-hmC sum score of hmeDIP-seq around active enhancer (± 200 bp) is reduced to one-fifth by *TET1* knockdown. P -values were measured using the Mann-Whitney U -test in (H) and (I). * $P < .05$; *** $P < .001$



3.3 | TET1 knockdown inhibits proliferation of hepatoma cell lines

To evaluate the role of TET1 in liver cancer, we introduced siRNAs targeting *TET1* into HepG2 and Huh7 cells (Figure 3A). These two cell lines showed high expression level of *TET1* among the

Broad Institute Cancer Cell Line Encyclopedia (Figure S4). The transient knockdown of *TET1* resulted in a significant reduction of cell growth, indicating that TET1 promotes cell proliferation in liver cancer cells (Figure 3B). Immuno-dot blot assay showed a total decrease of 5-hmC after 48 hours of *TET1* suppression (Figure 3C). Subsequently, we assessed the effect of exogenous

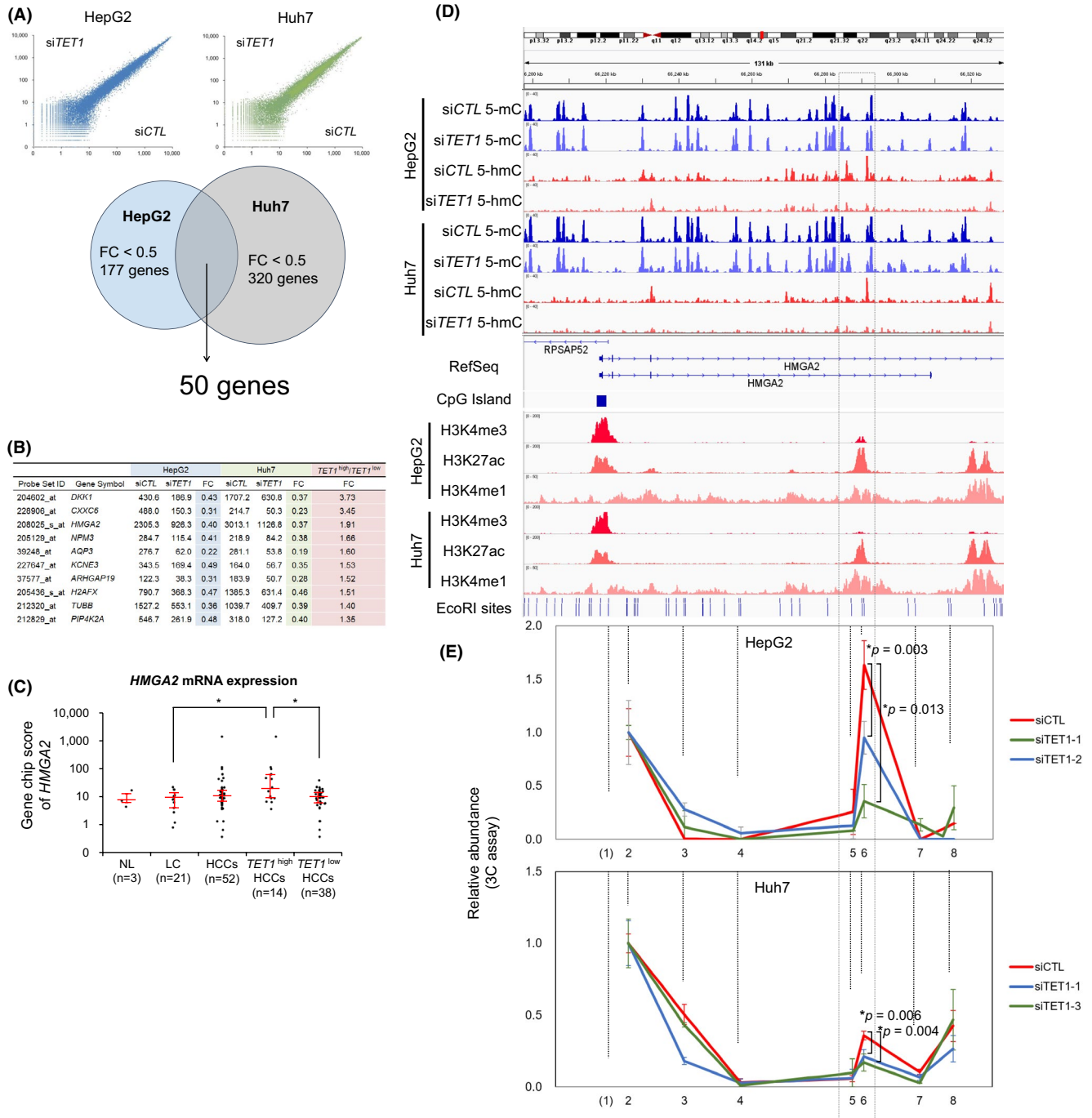


FIGURE 5 TET1 activates *HMGA2* through enhancer hydroxymethylation. **A**, Expression changes by *TET1* knockdown. Scatter plots (upper) demonstrate the GeneChip score of HepG2 (blue) and Huh7 (green). Venn diagram (lower) indicates the overlap of *TET1*-upregulated genes. **B**, Representative genes upregulated by *TET1*. **C**, *HMGA2* expression level among human clinical liver samples in expression microarray (U133 plus 2.0, Affymetrix). Each dot represents the GeneChip score of *HMGA2* (208025_s_at). Red line represents the median \pm quartile. **D**, The epigenetic statuses of the *HMGA2* locus showing cytosine methylation (blue, upper), hydroxymethylation (red, upper), and histone modification (lower) of HepG2 and Huh7 cells treated with siCTL and siTET1 on the Integrative Genomics Viewer (IGV). The dotted-line box intragenic enhancer regions identified by ChIP-seq analysis of liver cancer cells. **E**, 3C-qPCR analysis of long-distance interactions at the enhancer of *HMGA2*, in which 5-hmC was reduced by *TET1* knockdown in HepG2 and Huh7 cells. Data in (C) are shown as the median \pm quartile, and data in (E) are shown as the mean \pm SD from triplicate experiments. *P*-values were measured using the Mann-Whitney *U*-test in (C) and Student's *t*-test in (E). **P* < .05

overexpression via the HaloTag vector containing the full-length human *TET1* (Halo-TET1). The induction efficiency of Halo-TET1 and its enzymatic activity for methylcytosine oxidation were

confirmed (Figure 3D,E). The overexpression of Halo-TET1 rescued siRNA-mediated growth inhibition in HepG2 cells (Figure 3F). Taken together, our data demonstrate that *TET1* enhances cell

proliferation in liver cancer cells, suggesting that TET1 functions as an oncogenic regulator in human HCC.

3.4 | TET1 is involved in transcriptional regulation via cytosine demethylation at active promoters and enhancers

To elucidate the impact of *TET1* depletion on transcriptional regulation, we profiled the change of cytosine modifications along with the epigenomic status of the liver cancer cell lines. Compared with the histone modification statuses of HepG2 cells defined in the Encyclopedia of DNA Elements (ENCODE) project,³³ 5-hmC was preferentially enriched in enhancers (28.8%) and transcribed regions (27.1%), while 5-mC was distributed in heterochromatin (40.2%) and transcribed regions (35.5%) (Figure 4A). In active promoter regions, 5-mC and 5-hmC showed a bimodal modification pattern that spanned 2-3 kb with TSS at its center (Figure 4B,C, Figure S5). Although 5-mC showed no apparent changes, we found a remarkable 5-hmC decrease by *TET1* knockdown in active promoters and enhancers (Figure 4D-G). At active enhancer regions, 5-hmC mainly located at the center of enhancers, but 5-mC was depleted. These enhancer 5-hmC signals were decreased by *TET1* knockdown in HepG2 and Huh7 cells. Overall, the transcriptional activity was more affected by the level of cytosine hydroxymethylation in enhancers than in promoters. The changes of 5-hmC accumulation around active promoters did not affect gene expression (Figure 4H). On the other hand, 5-hmC reduction at active enhancers in *TET1* knockdown cells was significantly associated with decreased gene expression (Figure 4I). These results indicate that TET1-mediated enhancer hydroxymethylation may exert an impact on transcriptional regulation.

3.5 | Oncogenic target HMGA2 is dysregulated by TET1

The proliferative action of TET1 in liver cancer cells led us to consider that oncogenic target genes may be dysregulated by the aberrant deposition of 5-hmC. To explore such downstream targets, we studied the gene expression changes of *TET1* knockdown cells (Figure 5A). As a result, 177 and 320 genes were found to be downregulated (fold change < 0.5) by the transient knockdown of *TET1* in HepG2 and Huh7 cells, respectively. Among these, 50 genes were identified as common targets according to the expression ratio of *TET1*^{high} HCCs over *TET1*^{low} HCCs. Although there was no deposition of 5-hmC at the locus of the top-ranked gene, *DKK1*, several hmC peaks were observed at the *HMGA2* gene locus (Figure 5B).

The expression level of *HMGA2* in *TET1*^{high} HCCs was significantly higher than in *TET1*^{low} HCCs and in noncancerous liver tissues (Figure 5C). In the intronic region of *HMGA2*, we found the hyperhydroxymethylated region, which was diminished after

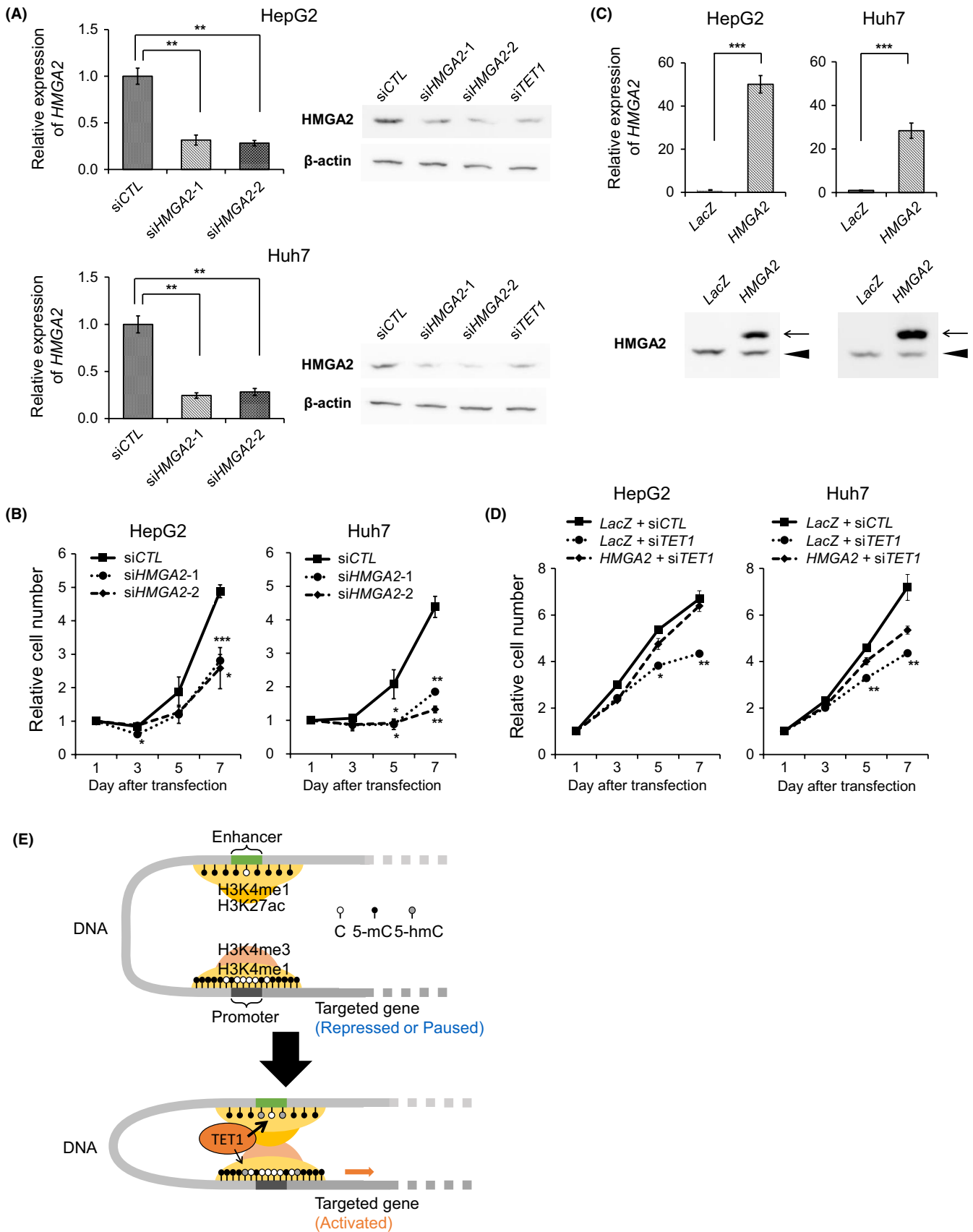
TET1 knockdown in both HepG2 and Huh7 cells (dotted-line box in Figure 5D). In *TET1*^{high} HCCs, unlike *TET1*^{low} HCC and nontumor samples, the intronic 5-hmC peak of *HMGA2* was observed in a similar way (Figure S6). ChIP-seq analyses of the hepatoma cell lines revealed that this region was marked with H3K27 acetylation and H3K4 monomethylation, known as active enhancer histone marks (Figure 5D, lower). Slight signals of H3K4 trimethylation were also implicated in the spatial interaction of this enhancer region to the promoter in vivo. We performed a 3C assay³⁴ and observed a specific interaction between the *HMGA2* promoter and this hydroxymethylated enhancer (Figure 5E, Figure S7). This promoter-enhancer interaction was validated by the Circularized Chromosome Conformation Capture (4C)-like view of the Hi-C data of HepG2 (Figure S8). Interestingly, this interaction was decreased by *TET1* knockdown in both cell lines. These results suggest that TET1-mediated hydroxymethylation plays an important role in the aberrant transcriptional activation of *HMGA2*.

To quantify the methylation levels of each CpG at the *HMGA2* enhancer regions, we performed multiplex targeted sequencing of BS-treated amplicons in the clinical liver samples. As shown in Figure S9, these CpGs were unmethylated in hESCs but were methylated in noncancerous liver tissues. In HCC tissues and liver cancer cell lines, this enhancer region was locally demethylated at the center of the H3K27ac peak. Compared with the epigenome profile in Roadmap Epigenomics data, the *HMGA2* locus was fully covered by the H3K27 trimethylation of the normal liver tissue (E066). However, these polycomb repressive complex marks disappeared in HepG2 cells (E118) and in H1 hESC (E003), and an active enhancer mark appeared upon NANOG and SOX2 binding (Figure S10). These data suggest that the epigenetic status of the intronic *HMGA2* enhancer is tightly regulated in a spatial and temporal manner.

Lastly, we analyzed the cellular effect of *HMGA2* knockdown to determine its role in liver cancer. Knockdown efficiency for suppressing *HMGA2* was verified by RT-qPCR and Western blotting (Figure 6A). As expected, *HMGA2* knockdown had an inhibitory effect on cell proliferation in HepG2 and Huh7 cells (Figure 6B). Next, we induced *HMGA2* overexpression by infecting pLenti6.3/V5 vector (Figure 6C). Cell proliferation assays showed that the overexpression of full-length *HMGA2* partially cancelled the growth inhibition of *TET1* knockdown in these cell lines (Figure 6D). Collectively, these results suggest that *HMGA2* is a major oncogenic target of TET1 via epigenetic mechanisms, an enhancer hydroxymethylation in HCC (Figure 6E).

4 | DISCUSSION

In this study, TET1 was demonstrated to play an oncogenic role in liver cancer cells. *TET1* upregulation was first revealed in a subgroup of HCCs presenting a hepatoblast-like gene expression pattern. Contrary to the reported finding of *TET1* in breast and prostate cancer,¹³ we found that TET1 promotes hepatoma cell proliferation. To



elucidate the oncogenic effectors regulated by TET1, we performed a genome-wide analysis of cytosine methylation and hydroxymethylation for TET1-upregulated HCCs. TET1 overexpression led to

global hyperhydroxymethylation, preferentially in active enhancer regions. Among them, we identified the specific enhancer hydroxymethylation in a putative oncogene, HMGA2.

FIGURE 6 TET1-targeted gene, *HMGA2*, enhances hepatoma cell proliferation. A, *HMGA2* expression of HepG2 and Huh7 cells with siCTL, *HMGA2* siRNA (si*HMGA2*-1 and -2), and si*TET1*. Left, relative *HMGA2* mRNA expression levels by RT-qPCR compared with cells with siCTL. Right, *HMGA2* expression by Western blotting analysis using anti-*HMGA2* antibody and anti- β -actin antibody. B, The tumor proliferation curves of HepG2 and Huh7 cells with siCTL and si*HMGA2* by WST-8. C, *HMGA2* expression of HepG2 and Huh7 cells with control (*LacZ*) and *HMGA2* overexpressed (*HMGA2*) by pLenti6.3/V5 vectors. Upper, relative *HMGA2* mRNA expressions by RT-qPCR compared with cells with *LacZ*. Lower, *HMGA2* expression by Western blotting analysis using anti-*HMGA2* antibody. Arrow and arrowhead indicate the overexpressed *HMGA2* proteins and endogenous *HMGA2* proteins, respectively. D, The tumor proliferation curves of HepG2 and Huh7 cells with siCTL, si*TET1*, *LacZ*, and *HMGA2* by WST-8. Data are shown as the mean \pm SD from triplicate experiments in (B) and (D). *P*-values were measured using Student's *t*-test. **P* < .05; ***P* < .01; ****P* < .001. E, Transcriptional regulation of oncogenic target *HMGA2* through enhancer cytosine hydroxymethylation, histone modification, and chromatin interaction

So far, TET1 has been described as a tumor suppressor in human cancers most likely due to its decreased expression levels and 5-hmC depletion in most cancer tissues.^{13,14,22,35-37} However, the expression level of TET1 in the previous reports was only verified by a limited number of cases or proven by semiquantitative antibody-based experiments, such as Western blot or immunohistochemical assay. Thus, we re-evaluated the *TET1* mRNA expression levels using thousands of cancer transcriptome data. As shown in Figure 1B, the expression pattern of *TET1* mRNA is cancer type-dependent. Generally, *TET1* expression levels are extremely high in hESCs compared with differentiated somatic cells.³⁸ Another TET family protein, TET2, showed the opposite pattern: higher expression in terminally differentiated somatic cells than in hESCs (Figure S1). Several studies have demonstrated that TET2 plays an essential role in hematopoietic differentiation.^{39,40} In addition, loss-of-function mutations of *TET2* have been reported in myeloid and lymphoid malignancies.^{9,39} In the context of solid cancer, there is a report of TET1 functions on tumorigenesis. Suppressive function for cell invasion was reported in prostate and breast cancers,¹³ consistent with the result of *TET1* downregulation in these types of cancer. In the present study, TET1 was upregulated in HCC and promoted cell proliferation of liver cancer cell lines, suggesting an oncogenic role in HCC development. Similarly, the potential oncogenic role of TET1 has been previously reported in several solid cancers, such as glioma,⁴¹ mixed-lineage leukemia-rearranged leukemia,¹⁶ triple-negative breast cancer,⁴² and lung cancer.⁴³ These findings indicate that TET1 can function either as an oncogene or as a tumor suppressor depending on the cellular context.

Next, we explored 5-mC and 5-hmC mapping in clinical liver tissues and liver cancer cell lines. Although TET1 regulates 5-hmC levels in transcriptional regulatory regions for murine ESCs,^{19,32,44} the significance of 5-hmC reduction at promoters or enhancers for gene regulation is poorly understood.^{19,32,35,45-48} Overall, 5-hmC is depleted at TSS regions but enriched at enhancer and transcribed regions. With regard to the gene expression, 5-hmC is preferentially enriched in the downstream regions of TSS, especially for highly expressed genes. *TET1* knockdown in hepatoma cells also shows the involvement of the cytosine demethylation at active promoters and enhancers. Notably, 5-hmC reduction at active enhancers is associated with a decrease in gene expression. Although the global content of 5-hmC is greatly

decreased in tumor cells in vivo and in vitro,¹²⁻¹⁴ whether the decreased content of 5-hmC is caused by the downregulation or inactivation of TET proteins requires further study. Pfeifer et al also pointed out that a decreased content of 5-hmC is not always associated with the activity of TET family proteins or Isocitrate dehydrogenase family proteins,⁴⁹ which play a role in the DNA demethylation pathway. As 5-hmC is not maintained by DNMT1 during DNA replication,⁵⁰ the frequency of cell divisions has a great impact on the 5-hmC levels, as well as on the enzymatic activity. Therefore, rather than the global amount of 5-hmC and 5-mC, their local distribution is thought to be much more important for epigenomic dysregulation via the aberrant expression of TET1.

Finally, we identified the *HMGA2* gene as one of the important targets of TET1-mediated enhancer hydroxymethylation during hepatocarcinogenesis. Although the oncogenic action of *HMGA2* in HCC has been studied previously,⁵¹⁻⁵³ it is not well understood how *HMGA2* is upregulated. Interestingly, the active enhancer mark, H3K27 acetylation, of this intronic region is observed only in a limited number of cell lines, such as H1ESC and HepG2, in the ENCODE database. Similarly, another ENCODE database (University of Washington) on DNase I hypersensitivity sites of 193 cell lines indicates that the open chromatin regions in *HMGA2* locus highly depend on cell type.

Taken together, these results provide an important insight into the context-dependent role of TET1 and 5-hmC in cancer biology. GSEA analysis indicates that *TET1*^{high} HCCs show a hepatoblast-like gene expression pattern. This subgroup of HCC is characterized by the overexpression of oncofetal genes^{29,54} and a clinically worse prognosis.²⁷ Therefore, targeting the ectopic expression of TET1 would provide a translational impact to overcome these aggressive types of liver cancer.

ACKNOWLEDGEMENTS

We thank Kaori Shiina, Hiroko Meguro, and Saori Kawanabe for their technical assistance in the experiments, and Ryota Yamanaka for his assistance with data processing. This work was supported by a Grant-in-Aid for Scientific Research (S) (24221011) (HA) and a Grant-in-Aid for Young Scientists (B) (25860521) (GN) from the Ministry of Education, Culture, Sports, Science and Technology (MEXT), Japan, and the Program of Fundamental Studies in Health Sciences of the National Institute of Biomedical Innovation (NIBIO), Japan.

DISCLOSURE

The authors have no competing interest to declare.

ORCID

Genta Nagae  <https://orcid.org/0000-0002-2929-7990>

Shogo Yamamoto  <https://orcid.org/0000-0002-5564-2567>

Yutaka Midorikawa  <https://orcid.org/0000-0002-6662-0494>

REFERENCES

- Jones PA, Baylin SB. The fundamental role of epigenetic events in cancer. *Nat Rev Genet.* 2002;3:415-428.
- Jones PA, Baylin SB. The epigenomics of cancer. *Cell.* 2007;128:683-692.
- Baylin SB, Jones PA. A decade of exploring the cancer epigenome - biological and translational implications. *Nat Rev Cancer.* 2011;11:726-734.
- Esteller M. Cancer epigenomics: DNA methylomes and histone-modification maps. *Nat Rev Genet.* 2007;8:286-298.
- Chi P, Allis CD, Wang GG. Covalent histone modifications - miswritten, misinterpreted and mis-erased in human cancers. *Nat Rev Cancer.* 2010;10:457-469.
- Wilson BG, Roberts CW. SWI/SNF nucleosome remodellers and cancer. *Nat Rev Cancer.* 2011;11:481-492.
- Koh KP, Yabuuchi A, Rao S, et al. Tet1 and Tet2 regulate 5-hydroxymethylcytosine production and cell lineage specification in mouse embryonic stem cells. *Cell Stem Cell.* 2011;8:200-213.
- Yoo CB, Jones PA. Epigenetic therapy of cancer: past, present and future. *Nat Rev Drug Discov.* 2006;5:37-50.
- Shih AH, Abdel-Wahab O, Patel JP, Levine RL. The role of mutations in epigenetic regulators in myeloid malignancies. *Nat Rev Cancer.* 2012;12:599-612.
- Kriaucionis S, Heintz N. The nuclear DNA base 5-hydroxymethylcytosine is present in Purkinje neurons and the brain. *Science.* 2009;324:929-930.
- Tahiliani M, Koh KP, Shen Y, et al. Conversion of 5-methylcytosine to 5-hydroxymethylcytosine in mammalian DNA by MLL partner TET1. *Science.* 2009;324:930-935.
- Kudo Y, Tateishi K, Yamamoto K, et al. Loss of 5-hydroxymethylcytosine is accompanied with malignant cellular transformation. *Cancer Sci.* 2012;103:670-676.
- Hsu CH, Peng KL, Kang ML, et al. TET1 suppresses cancer invasion by activating the tissue inhibitors of metalloproteinases. *Cell Rep.* 2012;2:568-579.
- Liu C, Liu L, Chen X, et al. Decrease of 5-hydroxymethylcytosine is associated with progression of hepatocellular carcinoma through downregulation of TET1. *PLoS ONE.* 2013;8:e62828.
- Sun M, Song CX, Huang H, et al. HMGA2/TET1/HOXA9 signaling pathway regulates breast cancer growth and metastasis. *Proc Natl Acad Sci USA.* 2013;110:9920-9925.
- Huang H, Jiang X, Li Z, et al. TET1 plays an essential oncogenic role in MLL-rearranged leukemia. *Proc Natl Acad Sci USA.* 2013;110:11994-11999.
- Ito S, D'Alessio AC, Taranova OV, Hong K, Sowers LC, Zhang Y. Role of Tet proteins in 5mC to 5hmC conversion, ES-cell self-renewal and inner cell mass specification. *Nature.* 2010;466:1129-1133.
- Williams K, Christensen J, Pedersen MT, et al. TET1 and hydroxymethylcytosine in transcription and DNA methylation fidelity. *Nature.* 2011;473:343-348.
- Xu Y, Wu F, Tan L, et al. Genome-wide regulation of 5hmC, 5mC, and gene expression by Tet1 hydroxylase in mouse embryonic stem cells. *Mol Cell.* 2011;42:451-464.
- Kim R, Sheaffer KL, Choi I, Won KJ, Kaestner KH. Epigenetic regulation of intestinal stem cells by Tet1-mediated DNA hydroxymethylation. *Genes Dev.* 2016;30:2433-2442.
- Khoeiry R, Sohni A, Thienpont B, et al. Lineage-specific functions of TET1 in the postimplantation mouse embryo. *Nat Genet.* 2017;49:1061-1072.
- Jeschke J, Collignon E, Fuks F. Portraits of TET-mediated DNA hydroxymethylation in cancer. *Curr Opin Genet Dev.* 2016;36:16-26.
- Kimura H, Hayashi-Takanaka Y, Goto Y, Takizawa N, Nozaki N. The organization of histone H3 modifications as revealed by a panel of specific monoclonal antibodies. *Cell Struct Funct.* 2008;33:61-73.
- Kaneshiro K, Tsutsumi S, Tsuji S, Shirahige K, Aburatani H. An integrated map of p53-binding sites and histone modification in the human ENCODE regions. *Genomics.* 2007;89:178-188.
- Zhang Y, Liu T, Meyer CA, et al. Model-based analysis of ChIP-Seq (MACS). *Genome Biol.* 2008;9:R137.
- Rao SS, Huntley MH, Durand NC, et al. A 3D map of the human genome at kilobase resolution reveals principles of chromatin looping. *Cell.* 2014;159:1665-1680.
- Yong KJ, Chai L, Tenen TG. Oncofetal gene SALL4 in aggressive hepatocellular carcinoma. *N Engl J Med.* 2013;368:2266-2276.
- Cairo S, Armengol C, Reynies A, et al. Hepatic stem-like phenotype and interplay of Wnt/beta-catenin and Myc signaling in aggressive childhood liver cancer. *Cancer Cell.* 2008;14:471-484.
- Hoshida Y, Nijman SMB, Kobayashi M, et al. Integrative transcriptome analysis reveals common molecular subclasses of human hepatocellular carcinoma. *Cancer Res.* 2009;69:7385-7392.
- Yamashita T, Budhu A, Forgues M, Wang XW. Activation of hepatic stem cell marker EpCAM by Wnt-beta-catenin signaling in hepatocellular carcinoma. *Cancer Res.* 2007;67:10831-10839.
- Pastor WA, Pape UJ, Huang Y, et al. Genome-wide mapping of 5-hydroxymethylcytosine in embryonic stem cells. *Nature.* 2011;473:394-397.
- Wu H, D'Alessio AC, Ito S, et al. Dual functions of Tet1 in transcriptional regulation in mouse embryonic stem cells. *Nature.* 2011;473:389-393.
- Ernst J, Kheradpour P, Mikkelson TS, et al. Mapping and analysis of chromatin state dynamics in nine human cell types. *Nature.* 2011;473:43-49.
- Dekker J, Rippe K, Dekker M, Kleckner N. Capturing chromosome conformation. *Science.* 2002;295:1306-1311.
- Lian CG, Xu Y, Ceol C, et al. Loss of 5-hydroxymethylcytosine is an epigenetic hallmark of melanoma. *Cell.* 2012;150:1135-1146.
- Yang H, Liu Y, Bai F, et al. Tumor development is associated with decrease of TET gene expression and 5-methylcytosine hydroxylation. *Oncogene.* 2013;32:663-669.
- Cimmino L, Dawlaty MM, Ndiaye-Lobry D, et al. TET1 is a tumor suppressor of hematopoietic malignancy. *Nat Immunol.* 2015;16:653-+.
- Li W, Liu M. Distribution of 5-hydroxymethylcytosine in different human tissues. *J Nucleic Acids.* 2011;2011:870726.
- Quivoron C, Couronne L, Valle VD, et al. TET2 inactivation results in pleiotropic hematopoietic abnormalities in mouse and is a recurrent event during human lymphomagenesis. *Cancer Cell.* 2011;20:25-38.
- Moran-Crusio K, Reavie L, Shih A, et al. Tet2 loss leads to increased hematopoietic stem cell self-renewal and myeloid transformation. *Cancer Cell.* 2011;20:11-24.
- Takai H, Masuda K, Sato T, et al. 5-Hydroxymethylcytosine plays a critical role in glioblastomagenesis by recruiting the CHTOP-methylosome complex. *Cell Rep.* 2014;9:48-60.
- Good CR, Panjarian S, Kelly AD, et al. TET1-mediated hypomethylation activates oncogenic signaling in triple-negative breast cancer. *Cancer Res.* 2018;78:4126-4137.
- Filipcak PT, Leng S, Tellez CS, et al. p53-suppressed oncogene TET1 prevents cellular aging in lung cancer. *Cancer Res.* 2019;79:1758-1768.
- Yamaguchi S, Hong K, Liu R, et al. Tet1 controls meiosis by regulating meiotic gene expression. *Nature.* 2012;492:443-447.

45. Ficiz G, Branco MR, Seisenberger S, et al. Dynamic regulation of 5-hydroxymethylcytosine in mouse ES cells and during differentiation. *Nature*. 2011;473:398-402.
46. Cimmino L, Abdel-Wahab O, Levine RL, Aifantis I. TET family proteins and their role in stem cell differentiation and transformation. *Cell Stem Cell*. 2011;9:193-204.
47. Yu P, Xiao S, Xin X, et al. Spatiotemporal clustering of the epigenome reveals rules of dynamic gene regulation. *Genome Res*. 2013;23:352-364.
48. Tan L, Xiong L, Xu W, et al. Genome-wide comparison of DNA hydroxymethylation in mouse embryonic stem cells and neural progenitor cells by a new comparative hMeDIP-seq method. *Nucleic Acids Res*. 2013;41:e84.
49. Jin SG, Jiang Y, Qiu R, et al. 5-Hydroxymethylcytosine is strongly depleted in human cancers but its levels do not correlate with IDH1 mutations. *Cancer Res*. 2011;71:7360-7365.
50. Inoue A, Zhang Y. Replication-dependent loss of 5-hydroxymethylcytosine in mouse preimplantation embryos. *Science*. 2011;334:194.
51. Fusco A, Fedele M. Roles of HMGA proteins in cancer. *Nat Rev Cancer*. 2007;7:899-910.
52. Morishita A, Zaidi MR, Mitoro A, et al. HMGA2 is a driver of tumor metastasis. *Cancer Res*. 2013;73:4289-4299.
53. Wu L, Wang Z, Lu R, Jiang W. Expression of high mobility group A2 is associated with poor survival in hepatocellular carcinoma. *Pathol Oncol Res*. 2012;18:983-987.
54. Chiang DY, Villanueva A, Hoshida Y, et al. Focal gains of VEGFA and molecular classification of hepatocellular carcinoma. *Cancer Res*. 2008;68:6779-6788.

SUPPORTING INFORMATION

Additional supporting information may be found online in the Supporting Information section.

How to cite this article: Shirai K, Nagae G, Seki M, et al. TET1 upregulation drives cancer cell growth through aberrant enhancer hydroxymethylation of HMGA2 in hepatocellular carcinoma. *Cancer Sci*. 2021;112:2855-2869. <https://doi.org/10.1111/cas.14897>